

Pondermotive Wave
Forcing of Cosmic Plasma
with Addendum on
Climate Change and Dark
Matter Issues

Pondermotive Wave Forcing of Cosmic Plasma with Addendum on Climate Change and Dark Matter Issues

By

Rickard Lundin and Hans Lidgren

**Cambridge
Scholars
Publishing**



Pondermotive Wave Forcing of Cosmic Plasma with Addendum on Climate Change
and Dark Matter Issues

By Rickard Lundin and Hans Lidgren

This book first published 2025

Cambridge Scholars Publishing

Lady Stephenson Library, Newcastle upon Tyne, NE6 2PA, UK

British Library Cataloguing in Publication Data

A catalogue record for this book is available from the British Library

Copyright © 2025 by Rickard Lundin and Hans Lidgren

All rights for this book reserved. No part of this book may be reproduced, stored in a retrieval system, or transmitted, in any form or by any means, electronic, mechanical, photocopying, recording or otherwise, without the prior permission of the copyright owner.

ISBN: 978-1-0364-1692-8

ISBN (Ebook): 978-1-0364-1693-5

TABLE OF CONTENTS

Introduction.....	1
Chapter 1	4
Overview: Aurora and Space Plasma Physics	
Chapter 2	42
Plasma Acceleration and Ponderomotive Forces in the Cosmos	
Chapter 3	54
Selected Applications of Magnetic Moment Pumping	
Chapter 4	124
The Bidirectional Miller Force	
Chapter 5	153
Neutron Spallation, Neutron Capture, and Nuclide Transmutations	
Chapter 6	177
Sources and Loss Processes of Terrestrial Deuterium: Comets and Meteors	
Chapter 7	202
NSNC and the Gradual Decay of Earth's Internal Heat Source	
Chapter 8	225
Cosmic Rays and Climate: Temperature Proxies and Isotope Transmutations	
Chapter 9	259
Cosmic Implications of Ponderomotive Wave Forcing: Addendum	
Chapter 10	261
On the Solar Activity, Cosmic Ray Neutron Fluxes and their Implications for the Global Climate	

vi
Table of Contents

Chapter 11	293
Charge exchange Energetic Neutral Atom (ENA) winds over the Venus Polar region	
Chapter 12	305
Dark Matter versus Energetic Neutral Atoms in Cosmos	
Summary and Concluding Remarks regarding Chapters 10, 11 and 12	315
Summary, Epilogue, and Acknowledgements	319

INTRODUCTION

The cosmos and *the universe* are two notions that define the content and extension of space. The notion of *the universe*, i.e. all space and time and their content in a “cellular” structure (expanding/contracting?), is part of the twentieth century concept of general relativity in astronomy and astrophysics. Conversely, *the cosmos* is a process-oriented notion where space is not the limit. *The cosmos* may rather be defined as the wealth of physical (plasma and neutral) processes and interactions between planets, stars, galaxies, and their intermediate regions. This notion implies that interplanetary and interstellar space is not merely a dull vacuum: matter, neutrals, and plasma are omnipresent in space, albeit at times with tenuous densities of matter/plasma. Plasma physical processes may govern a large, if not the main fraction of phenomena in the cosmos. For instance, the acceleration and ejection of solar wind plasma and its subsequent interaction with planets, comets, and asteroids in our solar system can be expected to apply to other stars and planetary systems in the Milky Way galaxy, as well as in other galaxies.

The above implies that experimentalists and theoreticians in solar system plasma physics have a certain “comfort zone” compared to astronomers and astrophysicists. Cosmic plasma physics is mundane in this respect since the theoretical knowledge of space plasma physics has gradually evolved from a combination of in situ space plasma measurements and theory.

With a brief résumé of relevant results obtained from more than 60 years of in situ space plasma measurements, this book proceeds to examine several primary issues, including: the concept of wave ponderomotive forces and their relevance for cosmic plasma acceleration; examples of the applicability of wave ponderomotive forces; and the significance of magnetic moment pumping (MMP) for the solar-planetary plasma environment and further away. The latter includes remote objects such as magnetized stars and galaxies.

In terms of the applicability of the Miller force (Miller, 1958), the characteristic of changing force direction at resonance frequency (and with attraction below resonance) may be considered “enigmatic”. However, the latter, with research that was honored by the award of the Nobel Prize in Physics (Ashton, 2018), and other experimental findings, may be sufficient to call for an upgrade to the theory of gravity.

A useful benefit of the action of wave ponderomotive forcing is its ability to stimulate isotope/nuclear transmutations via the two-stage process of neutron spallation and neutron capture (NSNC). The first stage, neutron spallation, sees the acceleration/energization of nucleons up to spallation energy (E_s), followed by the release of neutrons (n) from said element, for example, ${}^2\text{H} + E_1 \rightarrow {}^1\text{H} + n$, where E_1 is the spallation energy of ${}^2\text{H}$. The neutrons released may be picked up by other elements, such as ${}^{35}\text{Cl} + n \rightarrow {}^{36}\text{Cl} + E_2$, where E_2 marks the excess energy ($E_2 = \Delta mc^2$) released from the binding mass Δm , from ${}^{35}\text{Cl}$ ($E_2 \approx 8 \cdot E_1$). Isotope transmutations are well-known processes, but sufficient capacity to effectively derive excess energy and become a major energy supplier is yet to be achieved.

However, there are “natural” processes that can produce huge amounts of energy through the NSNC process, such as the impact of comets/meteors on the Earth’s atmosphere (Ch. 6) producing excess power in the nuclear blast range. In one of these events, the Chelyabinsk meteor was found to be capable of producing an energy release corresponding to the combined energy of Hiroshima and Nagasaki.

Another natural NSNC process, which is slow yet powerful, may be the most important internal terrestrial heat source and is discussed in Ch. 7. The internal heat source is readily available and can be harvested via the drilling of deep holes and water heat exchangers. However, the global distribution of this technology is uneven, and its realization can also be problematic in regions of high volcanic activity.

A third NSNC case, discussed in Chapter 8, concerns the continuous bombardment of the Earth’s upper atmosphere by cosmic ray protons, which are energetic particles originating from the Sun, interstellar space, and external galaxies. Of relevance here is that this energetic proton collision in the Earth’s atmosphere leads to the production of deuterium and, eventually, also to energetic neutrons. Subsequent moderation (thermalization) of the neutrons in the altitude range 5-30 km leads to neutron capture by atmospheric elements such as ${}^{16}\text{O}$, ${}^{12}\text{C}$, and ${}^{14}\text{N}$. The neutron capture (NC) of the dominant element, nitrogen in ${}^{14}\text{N} + n \rightarrow {}^{15}\text{N} + E_2$, leads to excess atmospheric heat production by a factor of about 6 in the altitude range ≈ 5 -15 km. Excess heat production in the altitude range 5-

15 km stimulates the formation of clouds in the same manner as jet planes do when flying in this altitude range. The relation between enhanced cloud formations, the blocking of sunlight, and a cooler climate (ice age) is consistent with enhanced cosmic ray flux. For instance, the isotope ratios used in the precipitation model $^2\text{H}/\text{H}$ and $^{18}\text{O}/^{16}\text{O}$, are consistent with the neutron capture model of isotope shifts. The ultimate question is, therefore, whether widespread dense cloud cover would be sufficient for the outbreak of a glaciation period? If so, to what extent would the input of solar radiation be reduced? In the same chapter, we discuss the case of Venus and make a comparison with Earth; these two planets are entirely different in terms of atmospheric and surface/ground conditions, but alike in size and probably also in their early evolutionary pasts. An important difference between Earth and Venus is that Earth has an intrinsic magnetic field while Venus does not this fact makes the discussion of their different responses to cosmic ray particle precipitation interesting.

OVERVIEW: AURORA AND SPACE PLASMA PHYSICS

The aurora borealis, a shimmering colorful lightshow seen in the polar winter night sky (Fig. 1 (a)), has fascinated mankind throughout history and continues to fascinate to such an extent that it is a major tourist attraction in the north. For space scientists, the mystique of the aurora is long gone, but the fascination of what it represents from a general space science point of view remains. The polar aurora and space plasma physics are not just a specialist subject of interest for space plasma physicists; auroral physics has a much broader cosmic plasma context, as noted by Hannes Alfvén in the 1930s (e.g. Alfvén, 1958, 1976, 1981). Auroral emission lines and their related morphologies are also frequently found in astrophysical objects, and some are also characterized by rayed and discrete structures, as shown in Fig. 1 (b), which gives a Hubble Space Telescope image of Barnard's Meropé Nebula. In fact, the more data we accumulate about deep space, the more it becomes obvious that physical processes governing the aurora may be ubiquitous in the cosmos.



Fig. 1.1(a) Polar aurora display over Kiruna. (Courtesy of M. Yamauchi, IRF).

Fig. 1.1(b) Barnard's Merope Nebula, IC 349, taken by the Hubble Wide Field Camera (courtesy of G. Herbig and T. Simon, University of Hawaii).

Starting from a position as an anonymous discipline on the edge of other “big” sciences, auroral and space plasma physics has evolved into an important tool for understanding not only the solar system, but also the evolution of stars and galaxies across the cosmos.

While the history of auroral research dates back thousands of years, with the first notes on auroral events being made by Aristotle and his disciples, contemporary auroral research, connecting magnetic disturbances, charged particle precipitation, and the occurrence of the aurora, is a product of the twentieth century. A precursor of the connection between charged particles and the aurora came from theoretical computations of charged particle orbits in the Earth's magnetic dipole field made by the Norwegian Carl Størmer in 1907. Another Norwegian, Kristian Birkeland, achieved what could be considered the peak of Norwegian influence on auroral research in the early twentieth century through a series of laboratory terrella experiments. In the Birkeland terrella experiments, charged particles (electrons) were accelerated towards a magnetized terrella (“little earth”, a small model ball).

The most important contribution to auroral research made by Birkeland was, however, his hypothesis on the connection between field-aligned electric currents and the aurora. This idea spurred a scientific debate that lasted for more than 50 years until field-aligned currents were finally confirmed (Zmuda & Armstrong, 1974). Two major scientists, Sidney Chapman (against) and Hannes Alfvén (for), carried the debate further. Sidney Chapman was an eminent scientist who introduced several important theoretical concepts in contemporary magnetosphere physics. However, he also consistently denounced Birkeland’s work and ideas. Hannes Alfvén became a supporter of Birkeland and opposed Chapman, promoting, and extending the idea of field-aligned/Birkeland electric currents and introducing the theory of field-aligned electric fields. In the service of this and other theories, Alfvén fought a life-long battle and was drawn into many scientific controversies that took too long to resolve. Hannes Alfvén eventually turned out to be right about many issues (e.g. Lundin & Marklund, 1995), although the space plasma physics community continues to argue about ideal magneto hydrodynamics (MHD) and magnetic reconnection, processes that was forcefully resisted by Alfvén. Alfvén favored kinetic plasma physics and the electric current approach to describe magnetic perturbations and boundary conditions. Ironically, Alfvén himself originally invented the concept of ideal MHD.

1.1 Contemporary Space Plasma Physics

The Space Age marked a new era of direct in situ space measurements, leading to the resolution of many early twentieth century debates regarding the causes of the aurora and associated magnetic and electromagnetic disturbances. The advent of measuring particles and fields and other properties in the terrestrial space environment, using instruments on sounding rockets and satellites orbiting the Earth for high-altitude on-the-spot measurements of physical properties, made a big difference compared to past remote sensing methods. Perhaps the most important finding from the early days of space exploration was that the space environment between the solar system planets and the Sun is not just an empty zone of space/vacuum. Instead, the planetary space environment is characterized by a zoo of plasma physical processes governed by the radial outflow/escape of solar plasma—the solar wind.

The Sun is the main “controller” of the solar system, meaning that the orbital motion of planets and other celestial objects, in addition to being governed by the solar gravitational pull, are also affected by the solar electromagnetic radiation, the variable solar wind, and the eleven-year cycle of shifts in

magnetic polarity. More than sixty years of space missions have provided and are still providing an improved understanding of the Sun and solar activity and our understanding has moved from the idea of a middle age star with a surface temperature of around 5800 K to one of an intriguing and complex hot plasma corona with temperatures greater than 10^6 K (Fig. 1.2 (a)) promoting an outward expansion of solar wind plasma (Fig. 1.2 (b)).

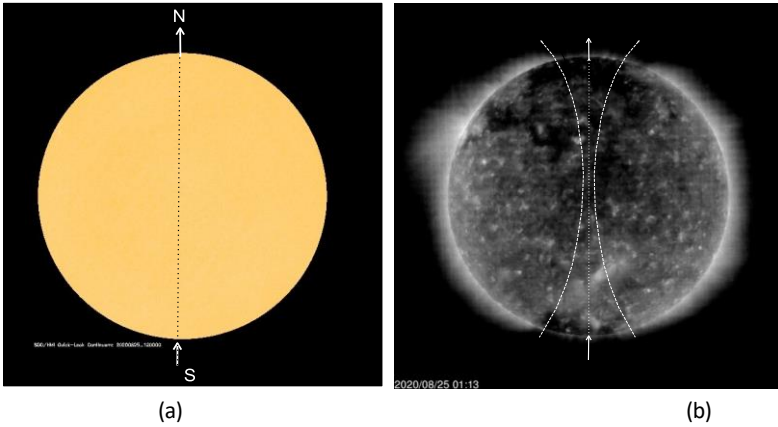


Fig. 1.2. SOHO images showing the solar surface (a) and the solar extreme ultraviolet (EUV) corona (b). The intense extreme EUV border (b) marks solar corona expansion—the solar wind. The dashed lines and arrows illustrate schematically the “average” magnetic dipole field during the 2020-08-25 solar minimums.

The scenarios in Fig. 1.2, illustrate the visible Sun versus the EUV composition of the Sun, present a seemingly enigmatic feature—a cooler surface with an extremely hot solar corona expanding outward on the surface, yet more modest for the polar regions. The cause of the enigma is discussed in more detail in Chapter 3.

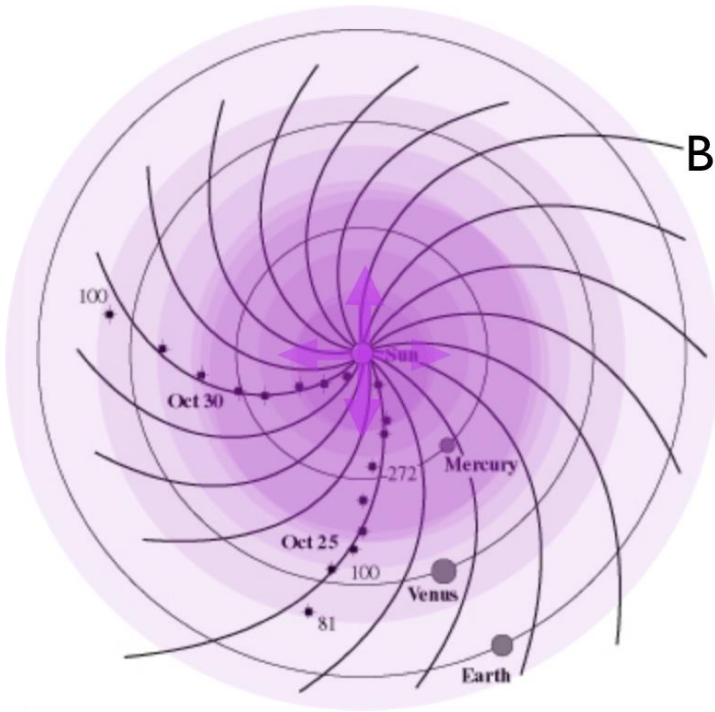


Fig. 1.3. Polar view of the solar magnetized plasma vortex. The curl of the magnetic field (B) evolves from the radial outward expansion of coronal plasma “frozen” in the solar magnetic field—the Parker spiral (Kenneth R. Lang 1994).

Magnetized plasma vortices, like those of solar wind expansion from the rotating Sun (Fig. 1.3), are common features in cosmic magnetized plasmas. The range of plasma vortex structures extends, from small-scale auroral vortices to large-scale galaxies.

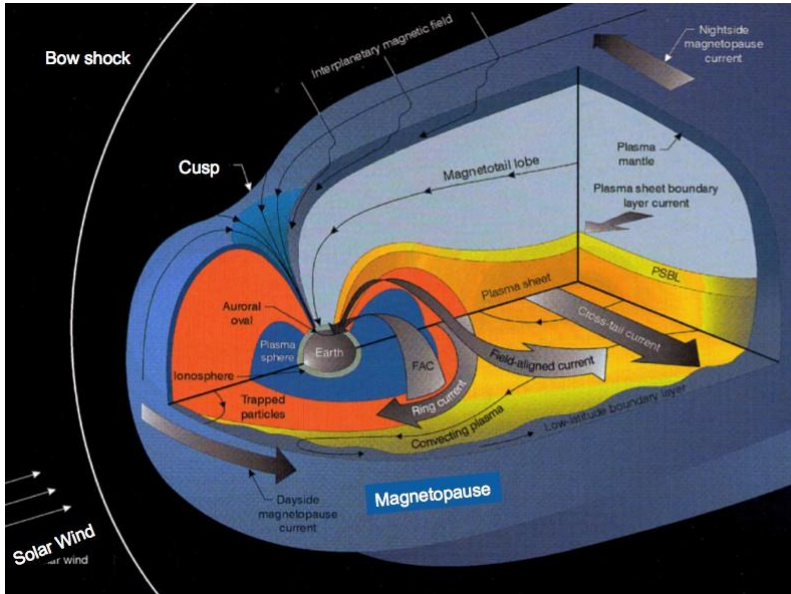


Fig. 1.4. Overview of the terrestrial magnetosphere derived from some 60 years of in situ plasma measurements. The collisionless bow shock marks the standoff distance to the free-flowing solar wind. The magnetopause is a region dominated by the Earth's magnetic field, inside of which the main solar wind energy and momentum transfer takes place (e.g. acceleration processes).

Figure 1.4 illustrates the planetary scale, the solar wind interaction with the terrestrial environment, and its atmosphere, ionosphere, and intrinsic magnetic field. The intrinsic control of the vortex is the Earth's magnetic field diverting the shock of solar wind plasma at the magnetopause. The transfer of solar wind energy and momentum to the magnetosphere, leading to a zoo of internal phenomena such as the aurora, takes place in the boundary layer inside the magnetopause. However, inner regions, such as the ring current and the radiation belt, are self-sustaining, governed by the Earth's intrinsic dipole magnetic field and thereby constituting the core of the plasma vortex. (For further details regarding magnetospheric plasma processes, see Chapter 3.)

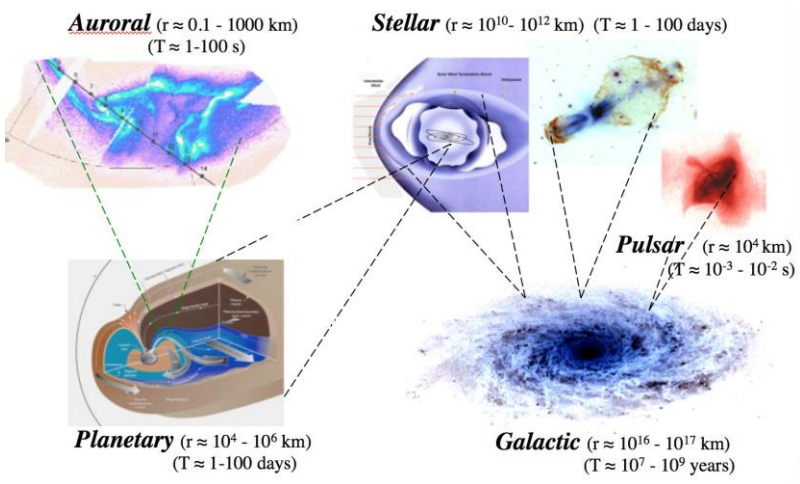


Fig. 1.5. Examples of cosmic plasma vortices, their sizes and rotation periods ranging from 0.1 to 10^{17} km and 1 second to 10^7 years, respectively.

Figure 1.5 presents a menu of cosmic objects characterized by intrinsically driven plasma vortices, with scales ranging from 0.1 to 10^{17} kilometers and rotation periods ranging from seconds to years. As for the latter, the largest type of plasma vortices in the cosmos is a galaxy.

Fig. 1.6 below shows the M51 galactic vortex in more detail. Note, for instance, the close coupling between the magnetic field (determined from polarization measurements) and the stellar material (stars, nebulas, and plasma environment) clearly demonstrating the close connection between the stellar plasma and the galactic magnetic field.



Fig. 1.6. The Whirlpool Galaxy M51 illustrating the close structural connection between the curled magnetic field (dashed lines) and the outflow of visible stellar/plasma material emerging from the central large scale magnetic vortex (black hole) of the galaxy. (Adapted from public domain material)

1.2 Auroral Particle Acceleration

The polar aurora is produced by the precipitation of energetic electrons, depositing their kinetic energy in the upper atmosphere/ionosphere whereby the excitation of local gas leads to light emissions. The process/excitation is like that found in a neon gas light tube, except somewhat more complex, comprising, for example, forbidden lines and delayed responses. A composite of the three auroral emission colors can be observed in Fig. 1.1 (a). Examples of emission lines include the green line oxygen emission O 5577 Å, the red O 6300 Å emission line, and the purple 8446 Å emission line.

The brightness, dynamics, and extension/banded structure of the aurora are directly connected to energetic electron precipitation along terrestrial magnetic field lines. However, because the source, the dynamo/ accelerator, may see rapid structural changes, equally dynamic variations of the aurora in time and space will result.

The imminent cause of dynamic changes in the Earth's auroral zone (Fig. 1.1(a)) is the interaction of solar wind with the Earth's magnetosphere (Fig. 1.4). The polar aurora, being a consequence of solar-terrestrial coupling, was already clear by the early twentieth century (e.g. Birkeland).

The breakthrough in auroral physics came with the first in situ space measurements from sounding rockets; the results were later verified by measurements from low Earth orbiting satellite experiments. Additionally, sounding rocket data evidence for a direct relation between particle precipitation and the aurora (McIlwain, 1960) was provided by later space measurements that proved the existence of parallel accelerating electric potentials, denoted "inverted Vs." (e.g. Frank & Ackerson, 1971; Evans et al., 1974; Shelley et al., 1976; Sharp et al., 1977), coexisting with field aligned Birkeland currents (Zmuda & Armstrong, 1974).

An example of the traversal of three inverted V auroral arcs over the polar region is displayed in Fig. 1.7. The energy peaks in the electron distribution, the "inverted V", in Fig. 1.7 indicate that the satellite crossed three upward-directed electric field potentials, manifested by narrow beams of downward-moving keV electrons.

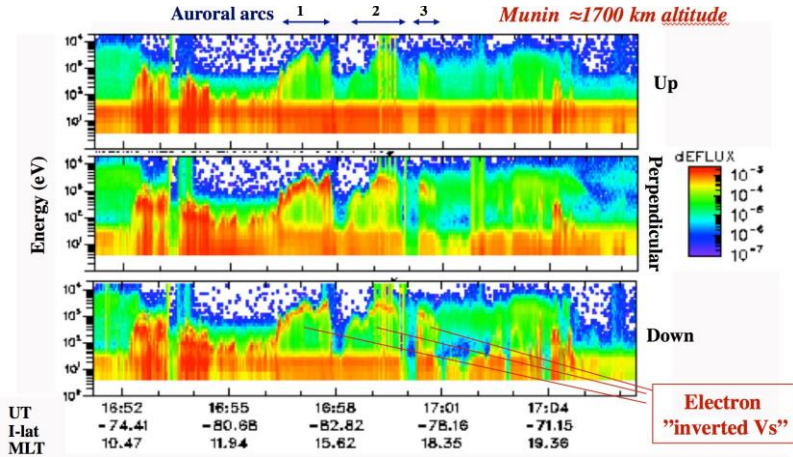


Fig. 1.7. Electron spectrometer data from the Swedish Nano satellite Munin traversing three inverted Vs, i.e. magnetic field-aligned electrostatic downward acceleration of electrons.

Further proof of the existence of parallel accelerating electric fields was found when mid-altitude satellites traversed what is now termed the “auroral acceleration region”. The fact that downward-accelerated electrons coincided with upward-accelerated positive ions confirmed the electrostatic behavior.

A diagram with satellite particle data illustrating the bidirectional flow of charged particles in a parallel electric field region is shown in Fig 1.8. The diagram also illustrates the magnetosphere dynamo required to power the auroral acceleration region and the associated Birkeland and closure currents of the electric dynamo.

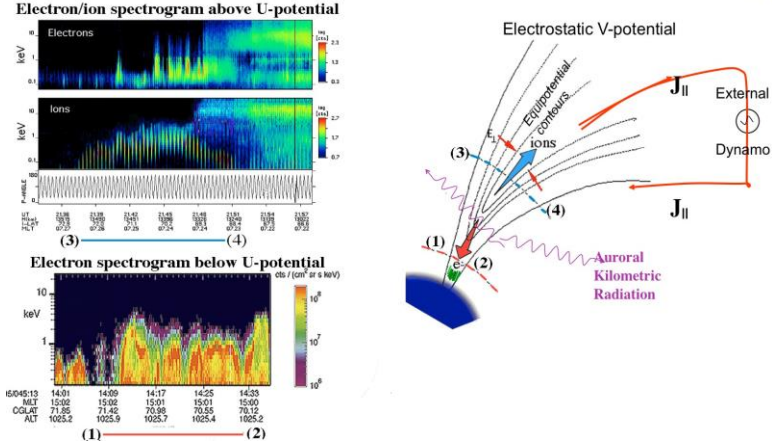


Figure 1.8. Diagram presentation of plasma acceleration in a quasi-electrostatic potential well driven by an external (solar wind) dynamo. The spectrogram on the left illustrates plasma data from a low-altitude satellite (1-2), showing downward-accelerated electrons, and data from a mid-altitude satellite, showing upward-accelerated ions (3-4).

Another aspect of planetary plasma outflow and escape, but now from the weakly magnetized planet Mars is illustrated in Fig. 1.9. Notice that the outflow energy in this case is essentially independent of mass, flowing outward in the same direction (MSO panel). This is the characteristic of non-magnetized objects, such as planet Venus and Comets. The outflow/escape is “tail-ward, governed by the solar wind dynamic flow. However, there are partially magnetized regions on Mars (Fig. 1.12) that marks a different story, i.e. magnetic field aligned acceleration over magnetic anomalies at Mars.

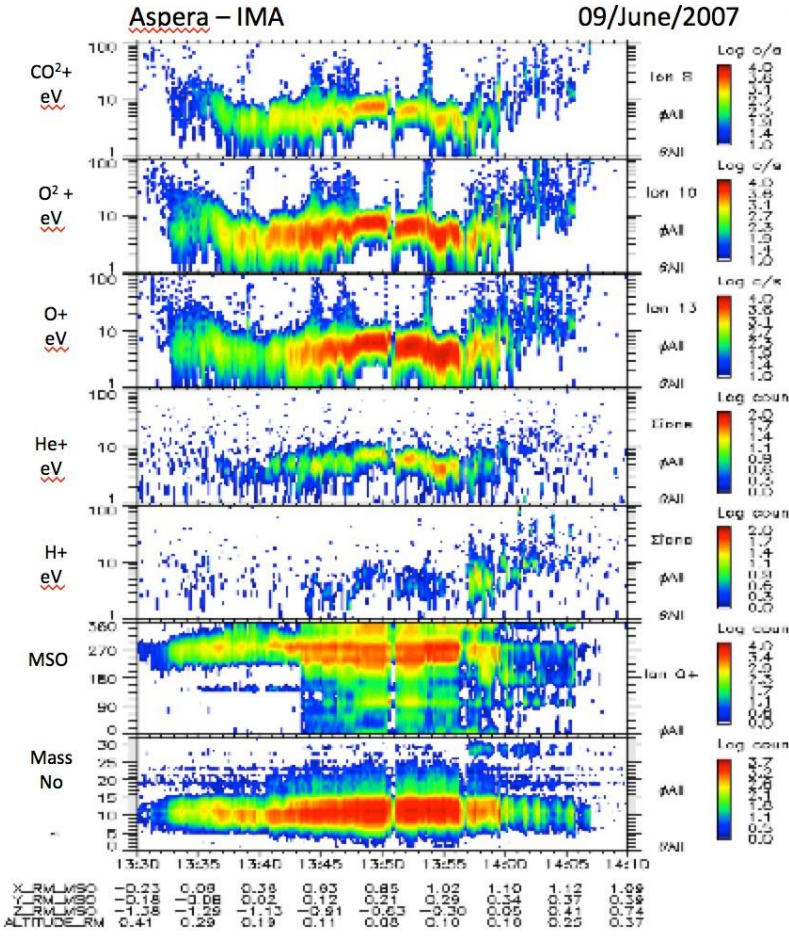
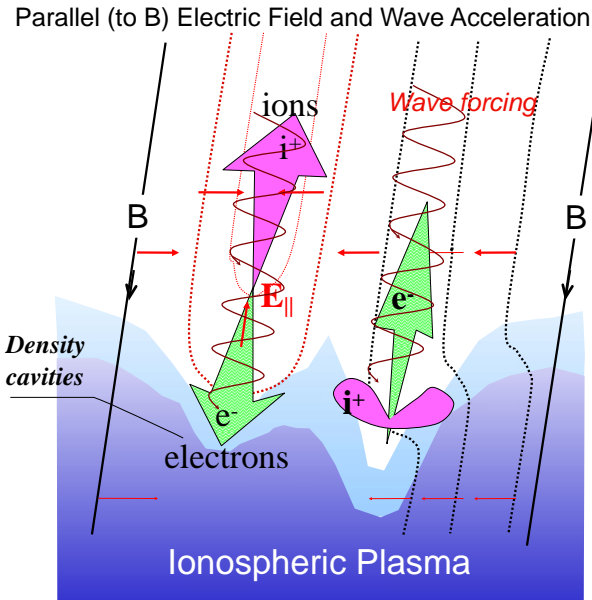


Fig. 1.9. Data from the Aspera Ion Mass Analyzer instrument showing the joint energization, outflow, and escape of ionospheric CO_2^+ , O_2^+ , O^+ , He^+ and H^+ ions from Mars.

For a long time, it was believed that significant parallel electric fields could only be sustained by sufficiently strong currents or within diverging magnetic fields, and then only as upward-directed electric fields in upward Birkeland currents. Today, we know that quasi-static field-aligned electric fields may also be directed downward (e.g. G. Marklund et al., 1994). This discovery marks, in a sense, the end of a long-standing dispute about field-

aligned electric fields that started with a paper by Alfvén in 1958. Quasi-electrostatic magnetic field-aligned electric fields may indeed occur, regardless of the magnetic field direction.

Hannes Alfvén was a proponent of the electric current circuitry analogy to understand solar wind-magnetosphere-ionosphere coupling. The current circuitry analogy simplifies many aspects of the auroral acceleration process, regarding the energy source (dynamo) and plasma acceleration (load). Figure 1.10 presents an illustration of how plasma acceleration, transversally as well as along magnetic field lines, is produced in connection with Birkeland currents connected to the topside ionosphere. Note in this figure that the excavation and outflow of ionospheric plasma may occur regardless of the electric current direction—upward in the electrostatic electron acceleration case, or downward/no current in the case of ponderomotive wave acceleration. More about ponderomotive wave forcing can be found in chapters 2 and 3.



Plasma acceleration $\mathbf{J} \cdot \mathbf{E} > 0$ (loading of external dynamo)
+ Ponderomotive wave forcing (charge neutral)

Fig. 1.10. Electric and magnetic field description of the auroral acceleration process. Note that heating and acceleration of ionosphere plasma implies either the loading of a magnetosphere dynamo ($\mathbf{J} \cdot \mathbf{E} > 0$), as a transfer of magnetosphere energy to the ionosphere plasma, or the charge neutral electrostatic/electromagnetic ponderomotive wave energization process (on the right) (Chapter 2).

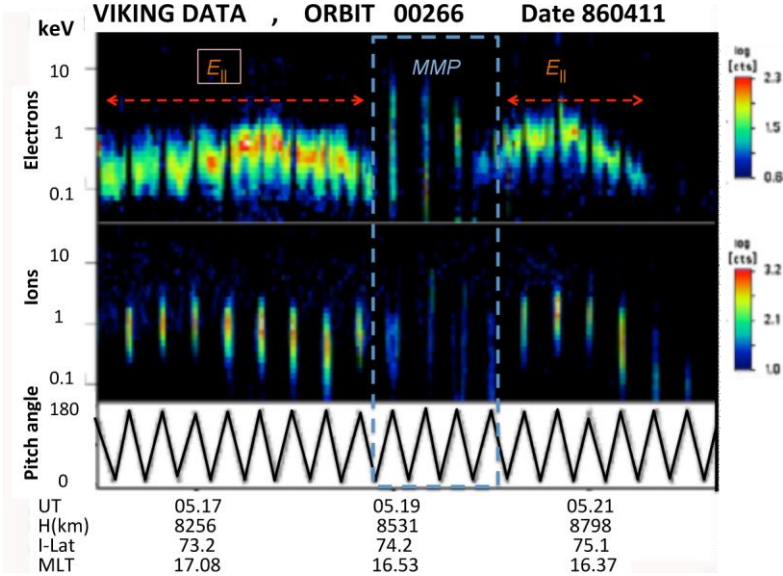


Fig. 1.11. Viking high altitude data from the traversal of the auroral acceleration region. $E_{||}$ marks regions with electrostatic field aligned acceleration of ions, $\approx 180^\circ$ pitch angle (upward) and electrons, 0° - $\approx 90^\circ$ pitch angle (downwards), electrons giving rise to an aurora. The vertical dashed box (MMP) marks a region with upward-accelerated ionospheric plasma—both ions and electrons are accelerated in the direction of the diverging polar region magnetic field.

Direct experimental evidence of the evacuation of ionospheric plasma at an altitude of about 1760 km is shown in Fig. 1.11. Note that the central region is characterized by a simultaneous upward acceleration (180° pitch angle) of both ions and electrons, the latter from a process denoted magnetic moment pumping (MMP), one of four ponderomotive forces discussed in chapters 2 and 3. MMP wave forcing is a charge neutral process in the sense that plasma accelerates in the direction of the magnetic field divergence. On the other hand, we have electrostatic acceleration by an electrostatic potential difference ($U=E_{||}Z_0$), where U is the electrostatic potential difference corresponding to a ≈ 2 kV maximum in the two cases in Fig. 1.11 and Z_0 is the vertical distance along the magnetic field line. The opposite flow directions of ions and electrons ($\approx 0^\circ$ - 90°) implies an upward-moving magnetic field-aligned current in the upward-directed $E_{||}$ sector.

1.3 Auroras on Other Planets in the Solar System

The conditions required for producing auroral light, Fig. 1.1(a) are like those found in the neon light-tube energetic electron excitation of a low-pressure gas (<30 mbar). However, for a discrete arc-like aurora, an additional condition is required, that of an intrinsic planetary magnetic field. All planets in the solar system with an atmosphere and a sufficiently strong intrinsic magnetic field fulfill this condition including Earth, Mars (magnetic anomalies), Jupiter, Saturn, Uranus, and Neptune.

As for Mars, images like that in Fig. 1.1 of a discrete aurora are not yet available. However, narrow structures of light emissions recorded photo metrically, simultaneous with downward-accelerated electrons and upward-accelerated ions (Lundin et al., 2006), are proof of the existence of a Martian aurora. Figure 1.12 shows data illustrating the classical energy-time characteristics of ions and electrons for spacecraft traversing U-shaped electric field potential structures associated with discrete auroras. Note in the lower panel that the combined electron and ion acceleration potential remained relatively stable at ≈ 400 V over a period of 40 minutes. The dip down to 50 V for electrons on both sides indicates a skewed, in and out, traversal of the main ≈ 400 V acceleration region over a period of 40 minutes.

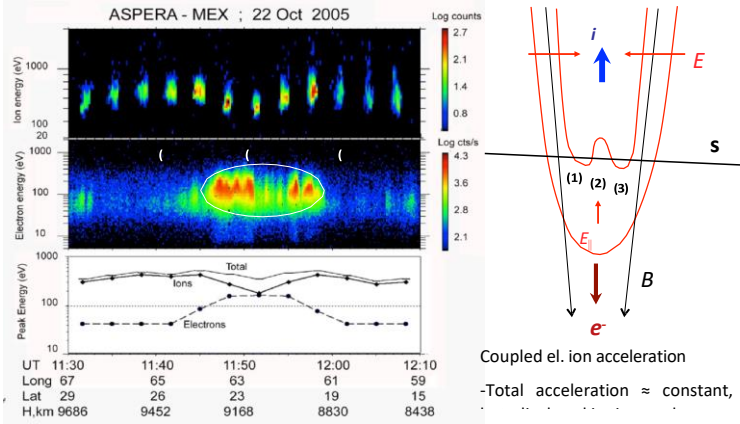


Fig. 1.12. Mars Express ion and electron energy-time spectra of magnetic field-aligned electron (downward) and ion (upward) acceleration associated with the traversal of a discrete aurora above a magnetic anomaly. The diagram on the right in Fig. 1.12 illustrates schematically the spacecraft (SC) traversal of the downward-oriented magnetic field and the upward/transverse U- shaped electric field structure.

1.4 Implications of Auroral plasma Acceleration and Erosion/Outflow

Having noted in the previous chapter that the aurora is associated with plasma acceleration and escape from the polar region, one may ask the question: what is the net loss of matter escaping the Earth's environment? The net escape rate has been a matter of some discussion and the outflow from the ionosphere is estimated to lie in the range 2-4 kg/s (e.g. Chappell et al., 1987). If the entire outflow escapes through the Earth's magnetotail, it represents a substantial loss of atmospheric constituents out into space, driving the comet-like behavior of the Earth. Figure 1.13 summarizes the context of the aurora and magnetic field-aligned plasma outflow, with a net loss corresponding to 80-250 tons/day. Although this loss may appear high, it represents only a small fraction of the Earth's atmosphere and hydrosphere: it would take some 50 billion years to evacuate the Earth's atmosphere at this rate, which is much longer than the lifetime of the solar system.

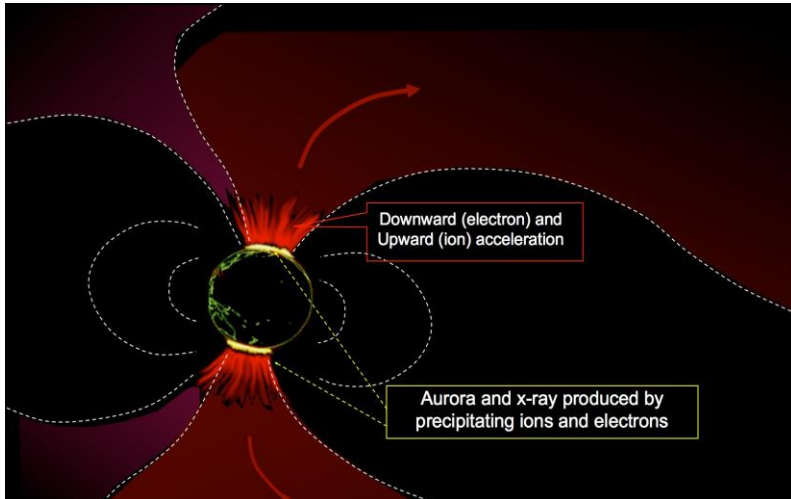


Fig. 1.13. Artist's conception of the Earth's polar region aurora due to electron acceleration and precipitation, together with the corresponding ionospheric plasma acceleration and escape.

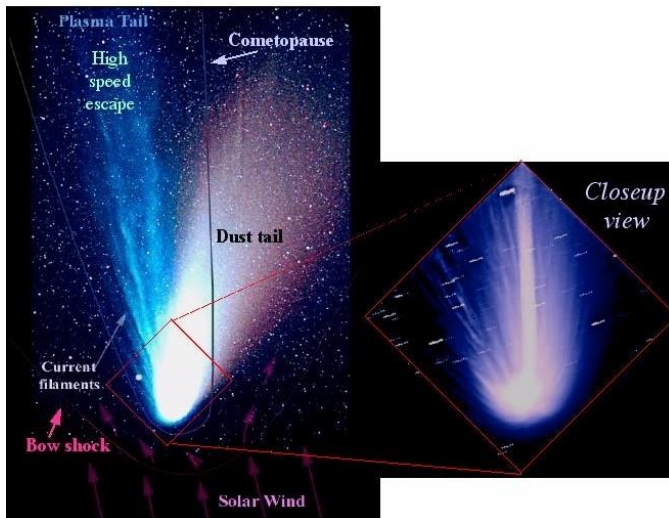


Fig.1.14 The Comet Hale-Bop. The two tails of Hale-Bop illustrate the two solar-induced atmospheric erosion processes: thermal escape (e.g. Jeans escape) and non- thermal escape (plasma escape). Note the filamentary structure of high-speed escape in the plasma tail.

While the Earth presents a rather stable celestial object, retaining a dense atmosphere and a substantial hydrosphere, comets are more vulnerable. Comets lose matter at rates that are orders of magnitude higher than the Earth during perihelion passes due to a combination of low gravity, high volatile content, and a lack of magnetic shielding. Comets are bright objects because of their atmospheric expansion and the formation of commentary tails by solar wind during solar approach. The solid core of a comet has a diameter in the range of a few kilometers or less and thus invisible to the naked eye. Comets like Hale-Bop (Fig. 1.14) well illustrate the combination of thermal and non-thermal escape. Thermal expansion results from the solar heating of volatile matter, with a fraction of that volatile matter having escape velocity. However, one may argue that the major fraction of matter being lost from a comet is due to solar wind forcing, i.e. non-thermal escape.

The long tails of comets consist of fast moving/high speed plasma accelerated to solar wind velocities. Note the filamentary characteristics of the plasma tail, which become even more pronounced in the close-up view of Fig. 1.14. Filaments and fine structures are characteristic of magnetized plasmas—these features are apparent in, for example, the aurora. Comet tail filaments are therefore related to the same processes as those of auroral acceleration and outflow of ionospheric plasma. Note also that the dust tail (Fig. 1.15), consisting of gas and debris expanding from the core along the comet orbit, shows filamentary features, indicating non-thermal escape also from the comet debris affected by the direction of the solar wind. Comet-like behavior, with the loss of atmosphere and ionosphere, can also be observed in the weakly magnetized planet Mars (Lundin et al., 1989) and the non-magnetized planet Venus (Barabash et al., 2007). Figure 1.15 demonstrates, however, that compared to Earth, Mars lacks a dipole magnetic field “umbrella” to fend off the solar wind and is therefore subjected to more direct solar wind scavenging of its atmosphere and hydrosphere.

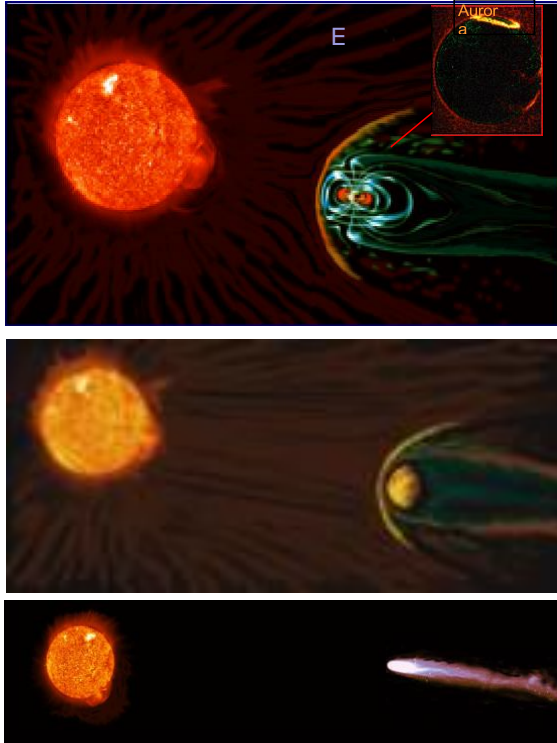


Fig.1.15. Solar wind forcing and the comet-like interaction with celestial objects in the solar system. Earth with magnetic dipole shielding; Mars and Venus with inadequate shielding; and comets are all subjected to direct solar wind forcing with heavy loss of volatiles.

The present volatile inventory of Mars is orders of magnitude lower than that of Earth, even considering the difference in size. However, besides the well-known water deposits in the polar regions, recent NASA high-resolution images suggest water deposits also exist at lower latitudes (Lauro et al., 2020). Considering that both planets were formed within the same (solar) nebula, possibly experiencing a rather similar history of debris accumulation, the question remains as to why they evolved so differently. A conceivable hypothesis is that Mars has lacked a magnetic shield to fend off the eroding solar wind for a significantly longer time.

Present estimates of the loss of volatiles over the 4.5-billion-year history of Mars indicate that this loss corresponds to some 12 meters of water distributed over the planet (Lammer et al., 2003). The lesson to take from this is that magnetized celestial bodies are better protected against external plasma forcing than non-magnetized bodies.

Like Mars, Venus, our sister planet closer to the sun, also lacks a strong intrinsic magnetic field to fend off the solar wind. Being close to the sun, the solar wind forcing on the topside atmosphere is about four times greater than found on Mars, but the gravity is strong enough to retain a dense atmosphere, primarily made up of CO₂. However, while Mars still has some water, Venus essentially has no water. Most likely, Venus was dehydrated by solar wind forcing in the same way as Mars, only more effectively. Figure 1.16 summarizes some aspects of atmosphere and hydrosphere evolution on Venus, Earth, and Mars.



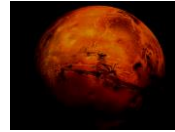
Venus

- Atmospheric density ≈ 90 times that of the Earth
- Mainly CO₂
- $t_{\text{Loss}} = ??$
- Lifetime of atm. ??



Earth

- ≈ 340 atm hydrosphere
- Mainly N₂ and O₂
- $S_{\text{Loss}} \approx 3 \text{ kg/s (O}^+, \text{H}^+)$
- Lifetime $t_{\text{atm}} \approx 50 \text{ By}$
- $t_{\text{hydrosphere}} \approx 26\,000 \text{ By}$



Mars

- Atmospheric density $\approx 1/100$ that of the Earth
- Mainly CO₂
- $S_{\text{Loss}} \approx 1 \text{ kg/s (O}^+, \text{H}^+)$
- Lifetime $t_{\text{atm}} \approx 100 \text{ My}$

Fig. 1.16 The atmospheres and hydrospheres on Venus, Earth, and Mars, and their evolution

The complexity of plasma erosion/outflow due to external forcing was briefly discussed in the previous section (figs. 4-6). While external forcing is, by definition, driven by an external energy source (e.g. waves, a dynamo etc.), internal forcing requires an internal energy source.

A star, such as our Sun, is a typical example. It is an internal energy source/dynamo capable of powering a closed current system, as described in Fig. 1.17, with upward acceleration and matter escape from the Sun. Note that electric current closure is provided in the outer portion of the stellar magnetosphere.

A more recent concept of the heliosphere is displayed in Fig. 1.18. The satellites Pioneer 11, Voyager 1, and Voyager 2 have all traversed the heliospheric magnetopause and entered the interstellar space regime. The main difference between figs. 1.17 and 1.18 is that the latter is topological, while the former emphasizes that the solar wind magnetic field in Alfvén's model is produced by an internal dynamo, the closed loop current system reaching out to the magnetopause with a return current reaching back to the Sun. In this way it resembles Earth's magnetosphere (Fig. 2.3) with plasma enclosed by a dipole magnetic field. On the other hand, Fig. 17 shows that the Sun is a star, not a planet, implying the existence of intrinsically produced plasma out to a boundary—the termination shock caused by an opposing galactic wind pushing the heliopause and the stellar wind (bow shock) further away from the Sun. The two systems, the solar and the interstellar, are apparently dynamic, implying highly temporal and spatial variations of the two intermediate boundaries.

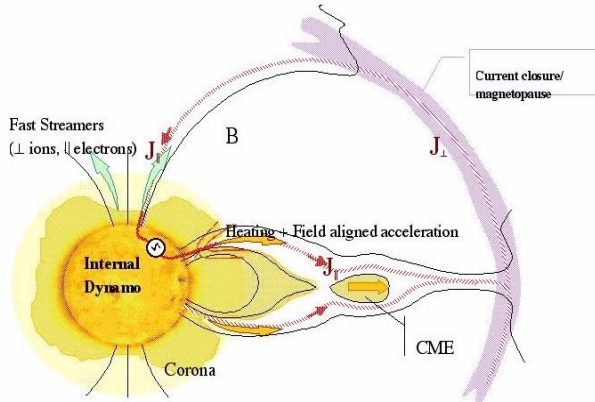


Fig. 1.17. A simplified current closure model of solar corona plasma expansion and escape driven by internal dynamo processes (Alfvén & Arrhenius, 1976).